

Parity-Dependence Potential for Composite Nuclei

著者	Yamaya T., Oh-ami S., Kotajima K., Seki H., Shinozuka T., Fujioka M.
journal or publication title	CYRIC annual report
volume	1988
page range	1-6
year	1988
URL	http://hdl.handle.net/10097/49447

I. 1. Parity-Dependence Potential for Composite Nuclei

Yamaya T., Oh-ami S., Kotajima K., Seki H.*, Shinozuka T.** and Fujioka M.***

*Department of Physics, Faculty of Science, Tohoku University
Department of Nuclear Engineering, Faculty of Engineering, Tohoku University*
Cyclotron and Radioisotope Center, Tohoku University***

One of interactions between complex nuclei reveals some characteristic feature which plays role of the Pauli exclusion principle. In microscopic studies on scattering between light nuclei, if a harmonic oscillator shell model with the same oscillator constant employed for descriptions of internal wave function of the constituent nuclei, the effect of the Pauli principle can be seen primarily to be expressed as an orthogonality condition to forbidden states for the relative motion, which is of short-range nature. As another effect, a core exchange term is known to be of a long-range nature and is expected to have distinctive contributions to parity dependent structures in the systems of two nearly identical nuclei. The experimental and the microscopic studies for this effect have been made in the scattering of $^3\text{He}+^4\text{He}$ and $^3\text{H}+^4\text{He}$ system of light nuclei by Brown and Tang.¹⁾ They have shown that scattering data from these system can be explained by the resonating group method and have derived effective local potential with parity dependence. Such an effect due to the Pauli principle is expected to appear on systems of heavier complex nuclei with a small mass difference.

In the present work, the parity-dependence potential in the $^{15}\text{N}+^{16}\text{O}$ and the $^{13}\text{C}+^{12}\text{C}$ scattering systems were examined experimentally, since the former system is expected to have molecular structure like $^{16}\text{O}+^{16}\text{O}$ in view of available number of freedom. Siemssen et al.²⁾ observed the gross structure of excitation functions from elastic scattering of ^{16}O from ^{15}N and pointed out a possibility of an elastic hole-transfer effect from its substructure at a large angle. Recently, Okabe³⁾ has been investigated for an interaction between ^{16}O and ^{15}N by the use of the resonating group method, especially, dependence of the interaction on spin and parity states are discussed. The latter system is also expected to have molecular structure like $^{12}\text{C}+^{12}\text{C}$ for a possibility of an elastic particle-transfer effect from the $^{13}\text{C}+^{12}\text{C}$ system. Von Oertzen et al.^{4,5)} have shown that this transfer process play a dominant role in the collision from analyses of the experimental data in term of the molecular two-state approximation and coupled-channel method. However, the

relationship between the transfer process and the core-exchange being a kinematical effect is not so clear enough.

A 85 MeV $^{15}\text{N}^{5+}$ ion beam and a 60 MeV $^{13}\text{C}^{4+}$ ion beam were provided from the Tohoku University's model-680 AVF cyclotron. The used targets were oxygen gas in pressure of 300 Torr and a self-supporting ^{12}C foil with a thickness of $100\ \mu\text{g}/\text{cm}^2$. The elastic cross sections were measured for angles $\theta_{\text{lab}} = 9.0^\circ\text{-}48.4^\circ$ with step of 0.7° in the scattering system $^{13}\text{C}+^{12}\text{C}$ and for angles $\theta_{\text{lab}} = 6^\circ\text{-}39.6^\circ$ with step of 0.7° in the scattering system $^{15}\text{N}+^{16}\text{O}$. Scattered ions and recoiling target nuclei were detected at same time and identified by use of $\Delta E\text{-}E$ telescope counter systems and the multi-data acquisition system.⁶⁾

The optical model calculations were made for the $^{13}\text{C}+^{12}\text{C}$ and the $^{15}\text{N}+^{16}\text{O}$ scattering systems using the computer code ELAST2.⁷⁾ An used optical model potential with the parity-dependence as follows;

$$V(r) = V^{\text{opt}}(r) + V^\pi(r)p^r,$$

where V^{opt} is the standard optical potential, V^π is the radial part of the parity-dependent potential and p^r is the Majorana exchange operator. In this model, V^π is a volume Woods-Saxon type. At the first, the parameters of the Woods-Saxon type potential for the only V^{opt} were automatically searched to reproduce the experimental data at the forward angles. The results of the DWBA calculations for the $^{13}\text{C}+^{12}\text{C}$ and the $^{15}\text{N}+^{16}\text{O}$ scattering systems are compared with the experimental data by the dotted curves in Figs. 1 and 2. These dotted curves cannot explain the large cross sections at the backward angles for both scattering systems. As the next step, the depth of the parity-dependent potential $V^\pi(r)$ were searched at all angles with the same geometrical parameters of the Woods-Saxon form as those of the V^{opt} . The results of calculations are shown with the solid and the dotted-dashed curves for $p^r = (-1)^l$ and $(-1)^{l+1}$, respectively, in Figs. 1 and 2. These curves well reproduced the data at all angles for both scattering systems. The obtained potential parameters are listed in Tables 1 and 2. It is to be noted that forward angular distributions are scarcely affected by V^π and interference between the forward and backward amplitudes are sensitive in p^r at intermediate angles for $^{13}\text{C}+^{12}\text{C}$ scattering system. In order to show a nature of the odd-even l -dependence for the parity-dependence potential V^π , the calculated phase shifts as a function of l are illustrated for both scattering systems in Figs. 3 and 4. For the $V^\pi = 0$, the phase shifts follows a smooth trend with respect to l in a region of nuclear surface. However, for the $V^\pi = 25\ \text{MeV}$ (and $30\ \text{MeV}$) the phase shifts of the systems show the zigzag patterns in a region of the nuclear surface in spite of using the volume type parity-dependence potential. Furthermore, to explain the effect of the parity-dependence potential at the backward angles, the behaviors of the scattering amplitudes at θ

= 180° in the case of $V^\pi = 0, +25$ and $+30$ MeV for both $^{13}\text{C}+^{12}\text{C}$ and $^{15}\text{N}+^{16}\text{O}$ systems, are shown as a vector sum of the partial wave amplitudes in Figs. 5 and 6. In the case $V^\pi = 0$ partial wave amplitudes cancel out each other. On the other hand in the case of $V^\pi = 25$ MeV (30 MeV) the changes of partial wave amplitudes cancel out each other for lower angular momentum but coherently contribute to give a rather large total scattering amplitude for the higher angular momentum in the nuclear surface region. A relation between the value of V^π and the backward enhancement is clearly shown in these figures.

References

- 1) Brown R. E. and Tang Y. C., Phys. Rev. 176 (1968) 1235.
- 2) Siemssen R. H., Fortune H. T., Malmin R., Richter A., Trippe J. W. and Singh P. P., Phys. Rev. Lett. 25 (1970) 536.
- 3) Okabe S., Prog. Theor. Phys. 68 (1982) 1790.
- 4) Oertzen W. von, and Bohlen H. G., Phys. Reports 19 (1975) 1.
- 5) Oertzen W. von, Imanishi B., Bohlen H. G., Treu W. and Voit H., Phys. Lett. 93B (1980) 21.
- 6) Satoh O., Yamaya T., Kotajima K. and Hasegawa K., Nucl. Instr. and Meth. in Phys. Resear. A268 (1988) 225.
- 7) Igarashi M., Institute for Nuclear Study, University of Tokyo Report No.PT-26, 1970.

Table 1. Parameters of optical potential $V^{\text{opt}}(r)$.

	E_{lab} (MeV)	V_R (MeV)	r_R (fm)	a_R (fm)	W_I (MeV)	r_I (fm)	a_I (fm)	r_C (fm)	x^2/N
$^{13}\text{C}+^{12}\text{C}$	60	79.13	1.183	0.470	11.10	1.380	0.149	1.35	10.5
$^{15}\text{N}+^{16}\text{O}$	81	101.7	1.153	0.510	41.73	1.210	0.499	1.25	39.4

$$*R_i = r_i(A_p^{1/3} + A_r^{1/3})$$

Table 2. Parameters of parity-dependence potential $V^\pi(r)$.

	V^π (MeV)	r^π (fm)	a^π (fm)
$^{13}\text{C}+^{12}\text{C}$	± 25.0	1.183	0.470
$^{15}\text{N}+^{16}\text{O}$	± 30.0	1.153	0.510

$$*R_i = r_i (A_p^{1/3} + A_r^{1/3})$$

Fig. 1

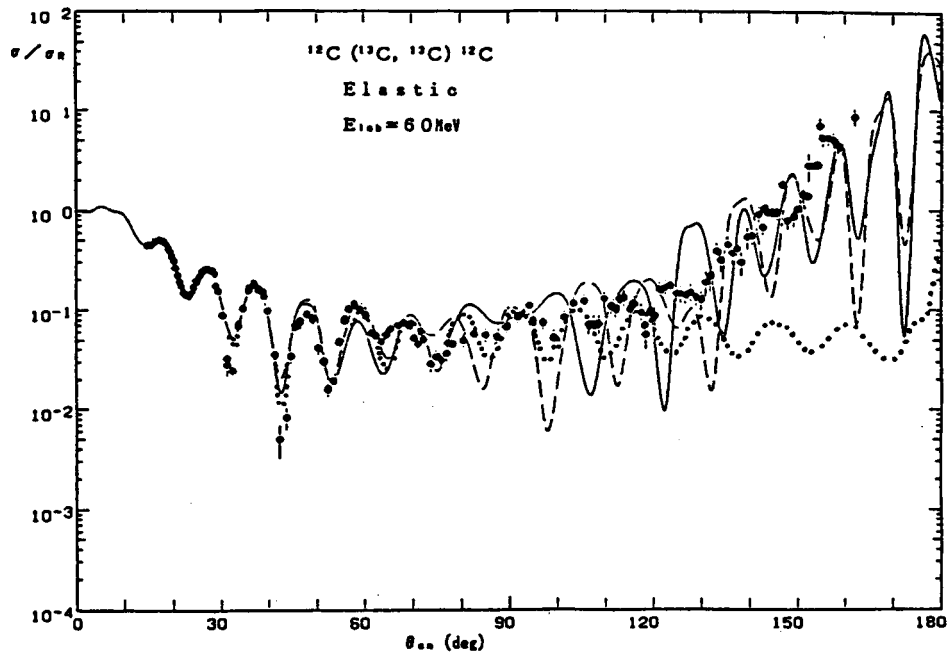


Fig. 2

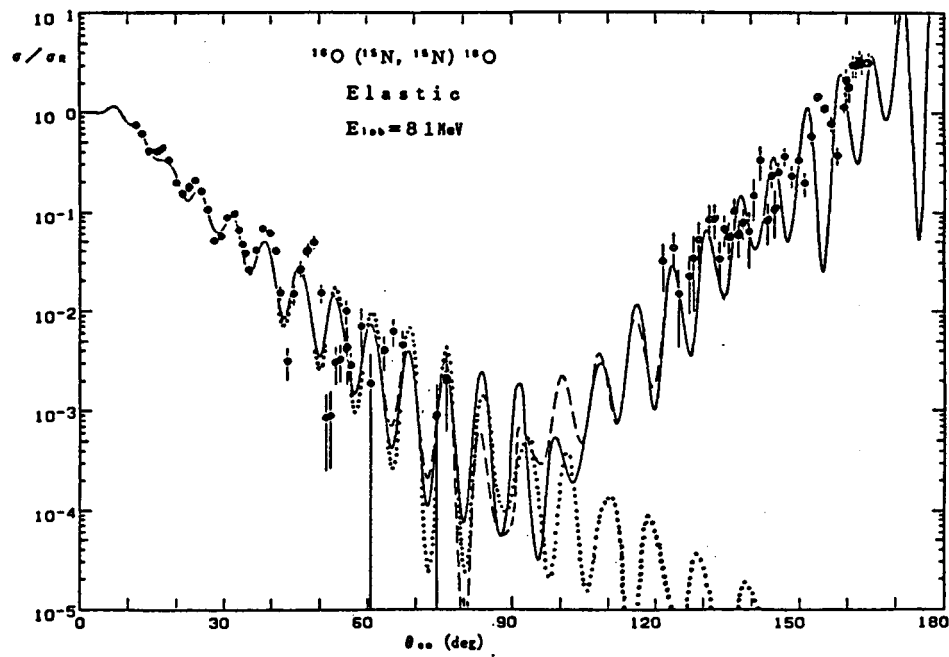


Fig. 1,2. Angular distributions of $^{13}\text{C}+^{12}\text{C}$ and $^{15}\text{N}+^{16}\text{O}$ scattering systems. The solid, the dash-dotted and the dotted curves indicate the best fit of the optical model calculations for $V^\pi = +25$ MeV (+30 MeV), -25 MeV (-30 MeV) and 0, respectively.

Fig. 3

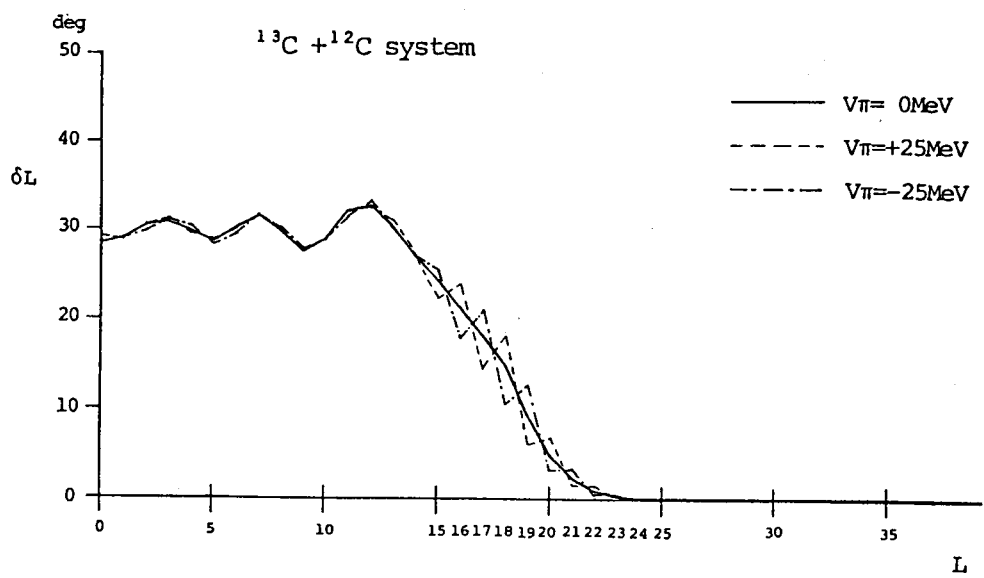


Fig. 4

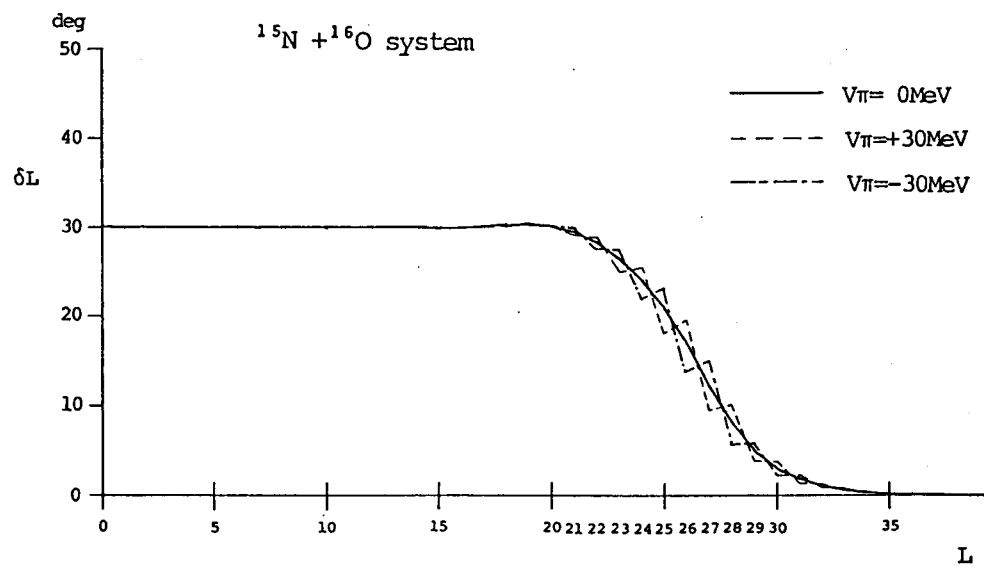


Fig. 3,4. Phase shift as a function of angular momentums of the scattered wave function.

Fig. 5

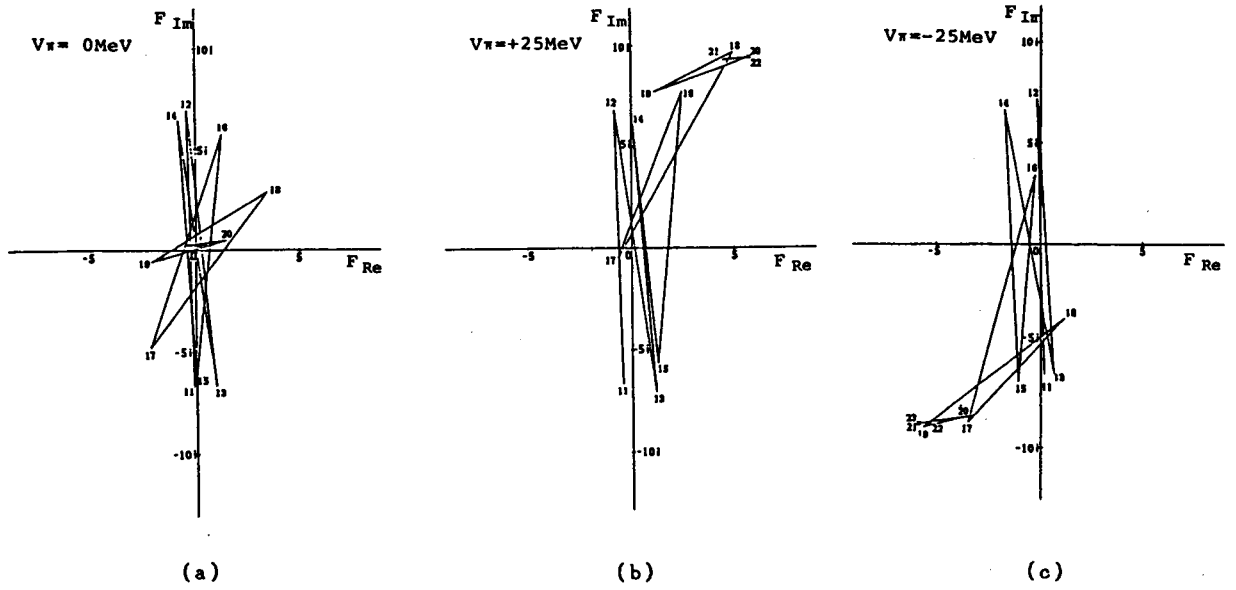


Fig. 6

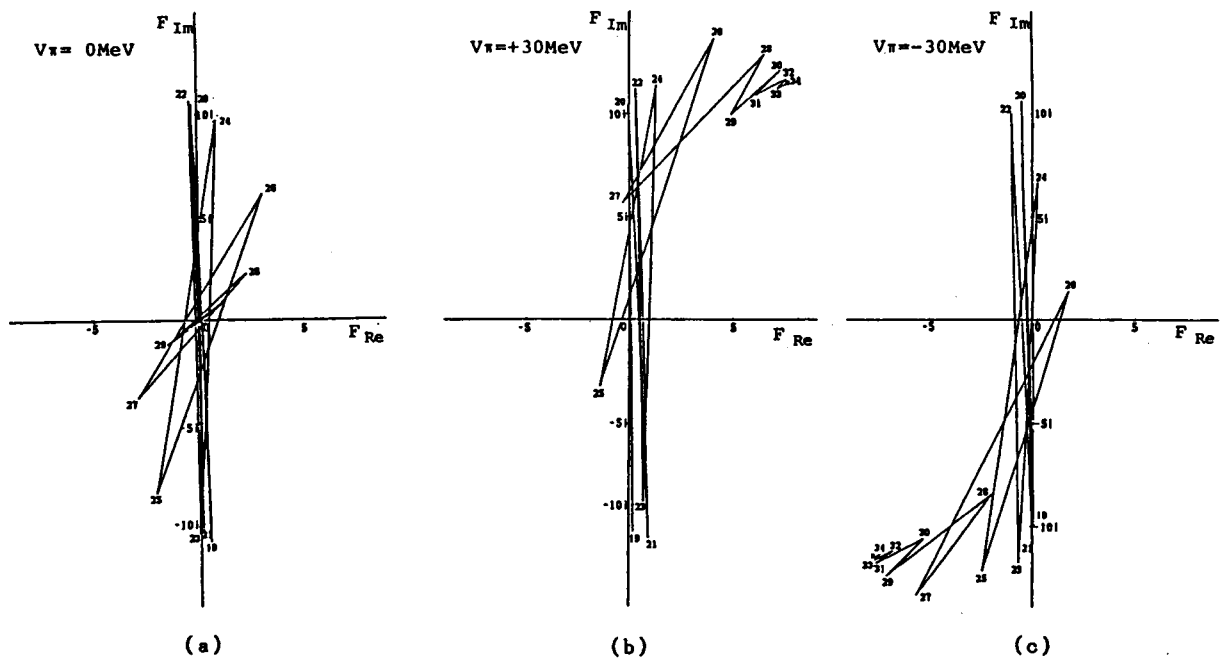


Fig. 5,6. Vector sum of the partial wave amplitudes at $\theta = 180^\circ$.